JOURNAL OF MATERIALS SCIENCE **37** (2002) 1951–1957

Morphological characterization of selectively overgrown GaN via lateral epitaxy

Y. G. WANG, Z. ZHANG
Beijing Laboratory of Electron Microscopy, Institute of Physics and Center for Condensed Matter Physics, Chinese Academy of Sciences, B.O. Box 2724, Beijing 100080, People's Republic of China
E-mail: ygwang@image.blem.ac.cn

V. P. DRAVID, P. KUNG, M. RAZEGHI
Department of Materials Science and Engineering, Northwestern University, 2225 N. Campus Drive, Evanston IL 60201, USA

Morphology as well as the dislocation networks in epitaxial GaN thin film, prepared via selectively lateral overgrowth has been characterized using TEM combined with focused ion beam (FIB) tool. The results showed that orientations of the sidewalls dependent on the orientations of mask strips. The sidewalls coincide with the $\{11\bar{2}1\}$ planes that form V type voids when the mask strips aligning along $\langle 1\bar{1}01\rangle$ directions and correspond to the $\{1\bar{1}00\}$ planes that result in rectangular voids if the strips arranging along the $\langle 11\bar{2}0\rangle$ directions. The dislocations were observed along the plan view direction. The dislocations in the lateral overgrown region mainly developed along the direction perpendicular to the strips. The genetic aspect of such morphologies of GaN films may have very close relation with the change of growing fronts of the epitaxial layer. © *2002 Kluwer Academic Publishers*

1. Introduction

GaN has attracted a lot of research attention because it has lower Ohmic contact resistance, large electron saturation velocity and a large breakdown field, combined with excellent thermal conductivity and stability, making it an excellent material for high-temperature, high-power and high-brightness optoelectronic devices such as field effect transistors (FET), junction, bipolar transistors and photodiodes etc [1–4]. Since threading dislocations resulting from large lattice mismatach and the difference between thermal expansion coefficients of epitaxial GaN and substrate severely degrade the optical and electric qualities of the GaN layer, high quality GaN is indeed required for manufacture of high performance optical device [5–7]. Laterally epitaxial overgrowth (LEO) has already been developed as a promising method for achieving high quality GaN, which is required for manufacture of high performance optical and electronic devices [8, 9]. The distribution and evolution of dislocation networks within LEO GaN layer have not been characterized in details due to difficult in preparation of plan view TEM samples at the specific positions, although there have been a lot of TEM observation on the microstructure of LEO GaN [10–15]. A study of morphology of LEO GaN and the dislocation networks within the overgrown region is essential for understanding the relationship between the synthesis, defect content and macroscopic properties of the GaN produced under a range of conditions.

Characterization of the microstructures of epitaxial GaN via selectively lateral overgrowth using TEM combined with FIB to prepare TEM plan view samples at specific positions is presented in this work with focus on fully understanding evolution of the morphology and dislocation distribution that occurred in the different growth situations in order for establishment of procession-microstructure-properties interrelations.

2. Materials and methods

A GaN layer of a thickness of 0.5 μm grown on a [0001] oriented sapphire wafer at the temperature of $\sim$450°C by a conventional metal organic vapor phase epitaxy (MOVPE) system using a horizontal quartz reactor having an inner diameter of 75 mm was used as a substrate. After an amorphous SiO_2 film of $\sim$0.5 μm deposited by MOVPE on the GaN substrate, mask strips with a width of 2 μm, 4 μm, 8 μm and 16 μm respectively aligned along the $[1\bar{1}00]$ and $[11\bar{2}0]$ directions, respectively, were fabricated by the stand photolithography with the purpose of reducing the threading dislocation density in the epitaxial GaN layer. A mask/window patterns with periods of 8 μm, 16 μm and 32 μm respectively were produced. Prior to the growth of thick GaN bulk, the surface was treated with acetone and alcohol in an ultrasonic cleaning bath, then the wafer was dipped into HCl solution. After being rinsed in deionized water, the substrate was dried in a nitrogen gas flow. MOPVE growth was performed at the temperature of 1100°C and a nitrogen pressure of 100 Torr. The GaN layer with different thickness was deposited for the same

mask/window patterns and pressure conditions. The cross sectional TEM specimens were made in order for revealing the morphology of the sidewalls. For characterization of the dislocation network in the over-grown region, plan view TEM specimens that proving a larger field for observation ware made by a Hitachi-2000A FIB operated at 30 kV. Initially, FIB milling was executed until the thickness of the slice reached less

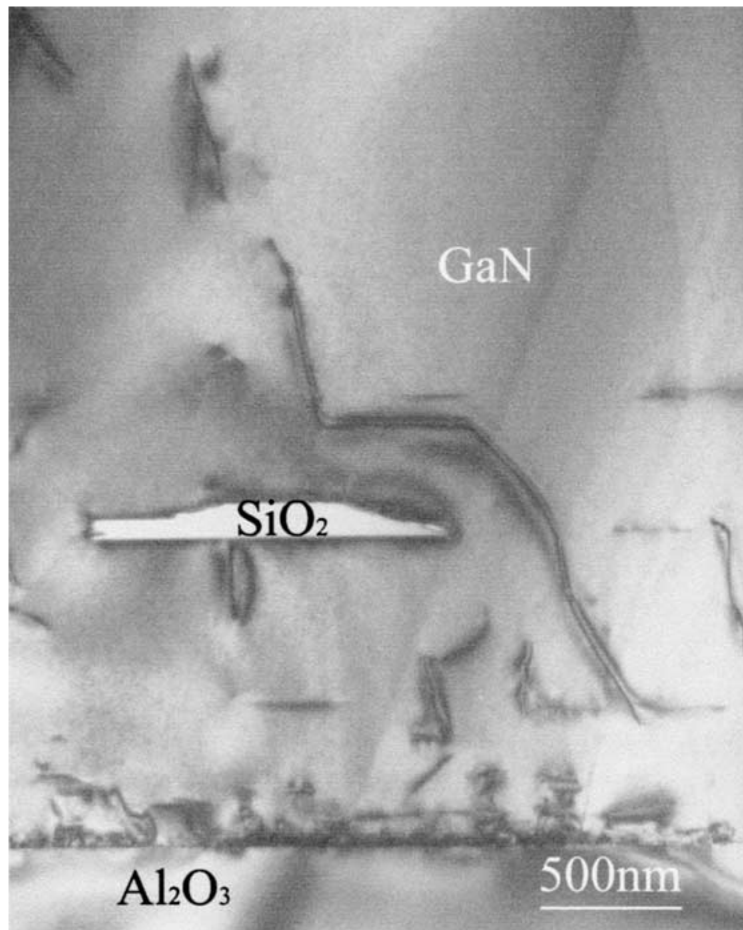

(a)

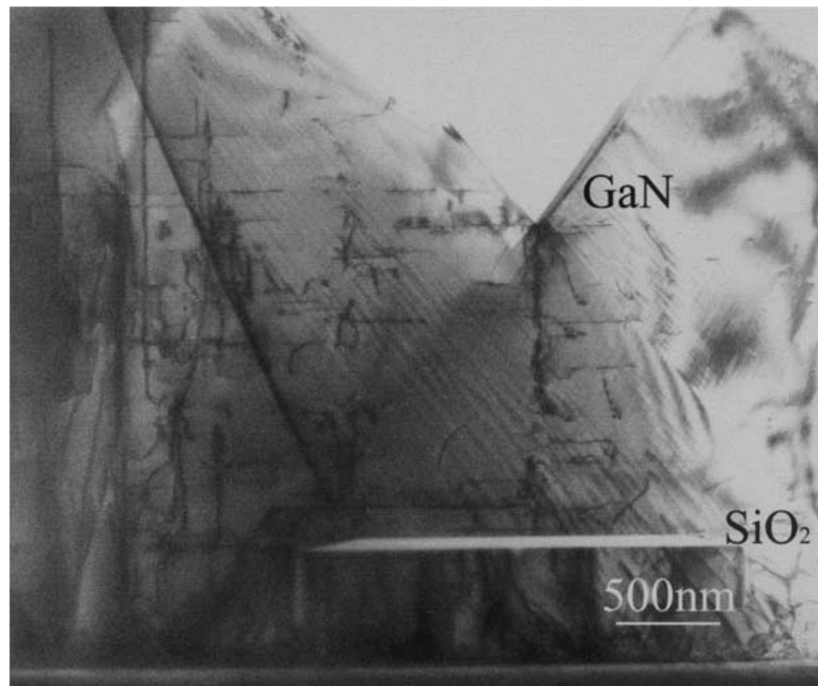

(b)

Figure 1 (a) and (b) are cross sectional TEM images showing morphology of two steps laterally overgrown GaN in the case of the mask strips, aligning along the $[1\bar{1}00]$ direction, with different width, (a) 2 micron, (b) 4 micron. The coalescence of LEO GaN occurred. (c) and (d) are SEM images demonstrating the sidewalls of epitaxial GaN for the strip with width of 8 micron (c) and 16 micron (d). The sidewalls are measured to be coincident with the $\{11\bar{2}1\}$ planes that result in the void of V-type configuration at the surface for the case of the strips with the width of 4, 8 and 16 micron. (*Continued.*)

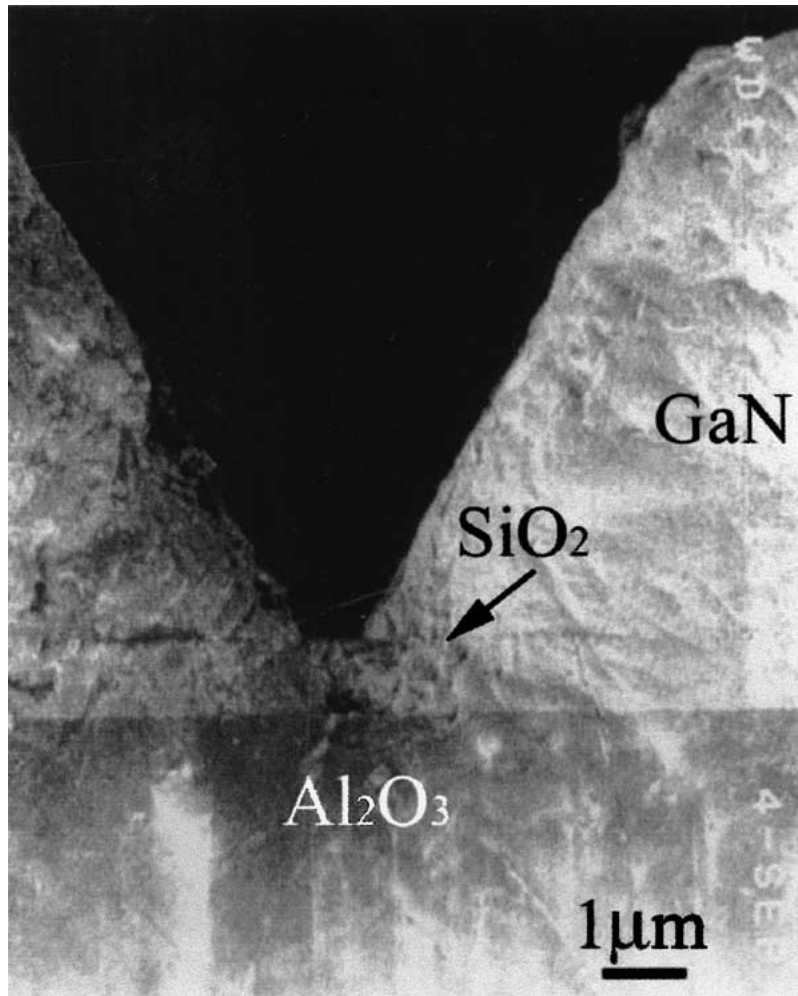

(c)

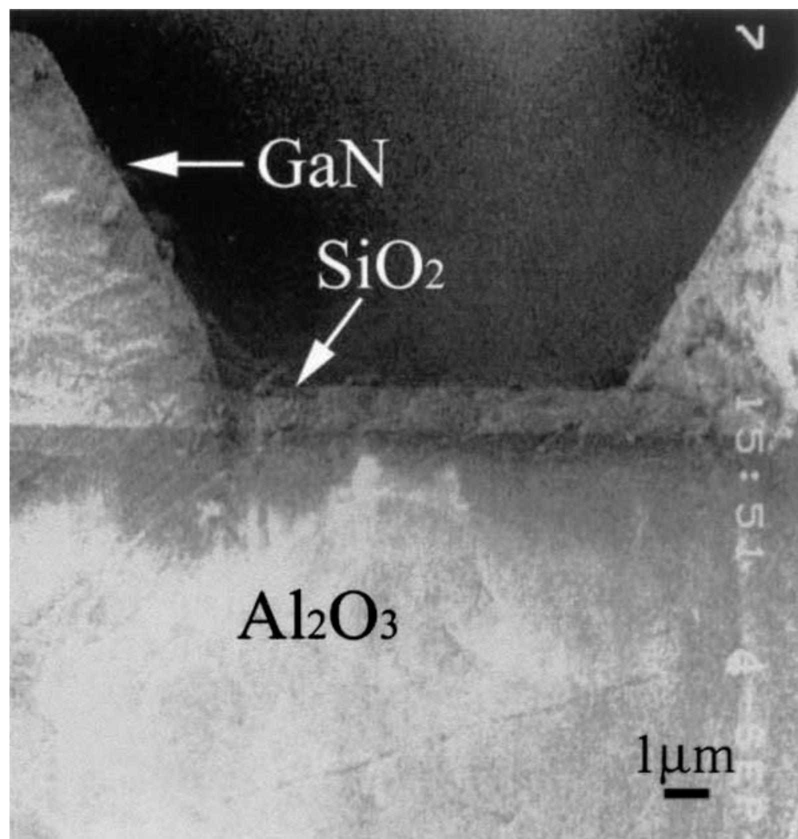

(d)

Figure 1 (*Continued.*)

than 0.1 μm under the condition that the incident angle of FIB was set vertical to the specimen surface with a beam current of 1 nA-100 pA. Finally, the incident angle of the ion beam was set to $\pm 2^\circ$ off the specimen normal by tilting the specimen in order for the thickness of the sample to be nearly uniform from top to bottom and a lower beam current was used [15].

A Hitachi-8100 electron microscope operated at 200 kV and a Hitachi-1500 SEM equipped with a field emission gun operated at 3–10 kV were used for characterization of the morphology of epitaxial GaN layers. The dislocation network located at specific positions and the corresponding dislocation density was estimated.

3. Results and discussion

3.1. Morphology of LEO GaN for mask strips aligning along the $\langle 1\bar{1}00 \rangle$ and $\langle 11\bar{2}0 \rangle$ directions respectively

GaN can nucleate in multiple tetrahedrally bonded polytypes, which could crystallize in either wurzite or zinc blende structure. It has been confirmed that the manufactured GaN has a wurzite structure based on the spectra of X-ray diffraction. Fig. 1a to b are the bright field images showing the morphology of LEO GaN with the mask strips aligning along the $[1\bar{1}00]$ direction. For the strip with a width of 2 micron the LEO GaN coalesced over the mask strip and no void formed. When the width of the strip increased to 4 micron, lateral growth fronts are convergent at the middle portion of SiO_2 strips and coalescence of the LEO GaN can be found, but the free surface formed a void with V-type configuration at the middle position of the strip. If elongating the growth time, the V-type void could be filled up to result in a smooth surface as that in Fig. 1a. For the strips with width of 8 and 16 micron as shown in Fig. 1c and d the LEO GaN did not coalesce. In all these cases the sidewalls are found to be coincident with the $\{11\bar{2}1\}$ planes, which means that the $\{11\bar{2}1\}$ planes may have lower energy than other planes, such as the $\{11\bar{2}0\}$ planes. The surfaces of the LEO GaN are {0001} and $\{11\bar{2}1\}$ planes, i.e. these two families of planes with minimum energies respectively.

Fig. 2a and b are bright field micrographs depicting a general view of the morphology of LEO GaN obtained under the same growth conditions as that in Fig. 1, but

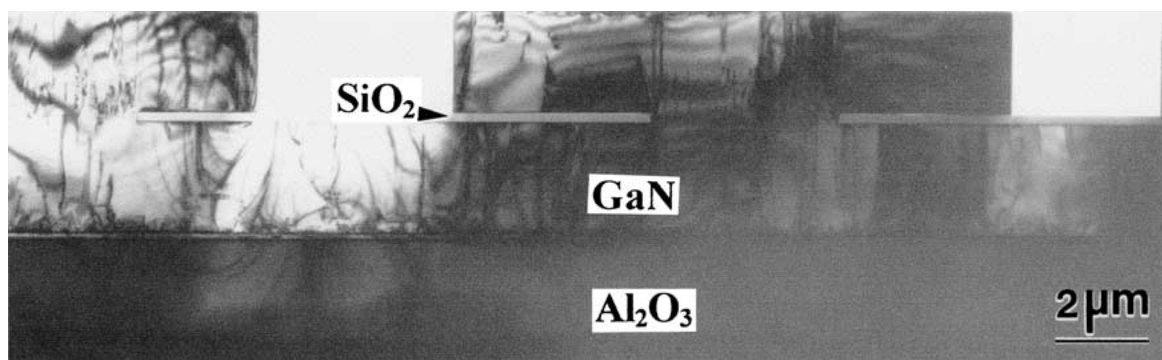

(a)

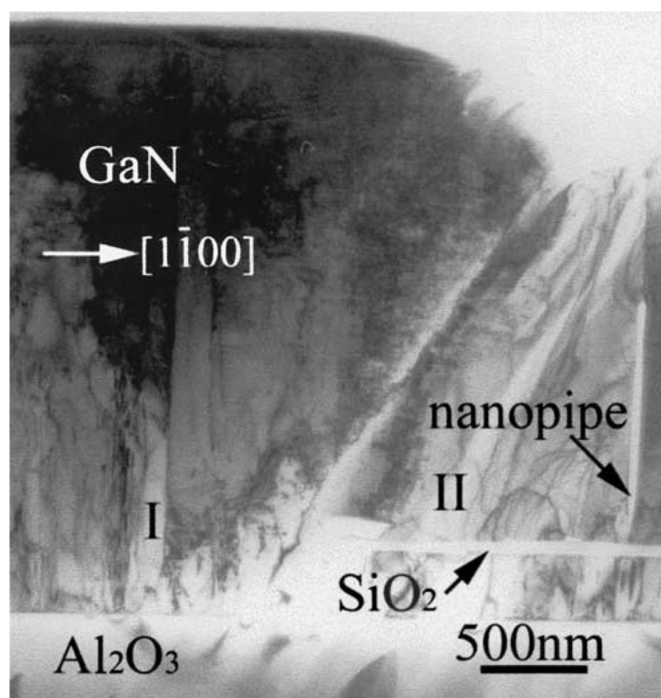

(b)

Figure 2 TEM micrographs depicting microstructures of LEO GaN for the strips aligning along the $[11\bar{2}0]$ direction, (a) 8 micron and (b) 4 micron. The sidewalls coincide with the $\{1\bar{1}00\}$ planes that introduce a rectangular void in (a) and result in a vertical nano-pipe with a length of $\sim$1.5 micron when the epitaxial GaN coalesced at the middle position of the strip in (b). The sites marked with I, II, are positions to be sampled with FIB for revealing dislocations networks within the masked region.

with the strips aligning along the ⟨11$\bar{2}$0⟩ directions.In Fig. 2a the LEO GaN did not merge over the strip and rectangular void formed. The sidewalls are found to coincide with the {1$\bar{1}$00} planes. The density of atoms at the {11$\bar{2}$0} planes is higher than other planes except {0001} planes. Thus, the surface of the LEO GaN are the {0001} and {11$\bar{2}$0} planes respectively. These two planes are the planes with the highest density of atoms in crystal with hexagonal symmetry. The growth fronts of the LEO GaN were along the ⟨0001⟩ and ⟨11$\bar{2}$0⟩ directions respectively. When the two ⟨11$\bar{2}$0⟩ growth fronts met, the coalescence of the LEO GaN could happen. In this case the growth front was along the ⟨0001⟩ direction. If the growth time was elongated as shown in Fig. 2b, where a vertical nano-pipe with a length of ∼1.5 micron is visible at the middle position of the strip. Because the sidewalls are vertical, the coalescence of LEO GaN occurred first at the top part when the sidewalls met with each other and left the bottom part un-contacted, as a result, the nano-pipe formed. The ratio of the LEO GaN growing along the horizontal and vertical directions can be calculated to be ∼1.5 : 1 based on Fig. 2a. This ratio could be adjusted by alternation of argon pressure. The results of the microstructural characterization of selectively overgrown GaN by TEM are shown in Table I for the SiO_2 masks aligning along both the ⟨1$\bar{1}$00⟩ and ⟨11$\bar{2}$0⟩ directions respectively.

3.2. Characterization of the dislocations in the LEO GaN

For analysis of the dislocation network in the overgrown region, Plan view TEM specimens, proving a larger field for characterization of the growth plane, ware made by FIB at the marked positions in Fig. 2b. Fig. 3a shows the corresponding bright field micrograph taken at I position in Fig. 2b.Threading dislocations

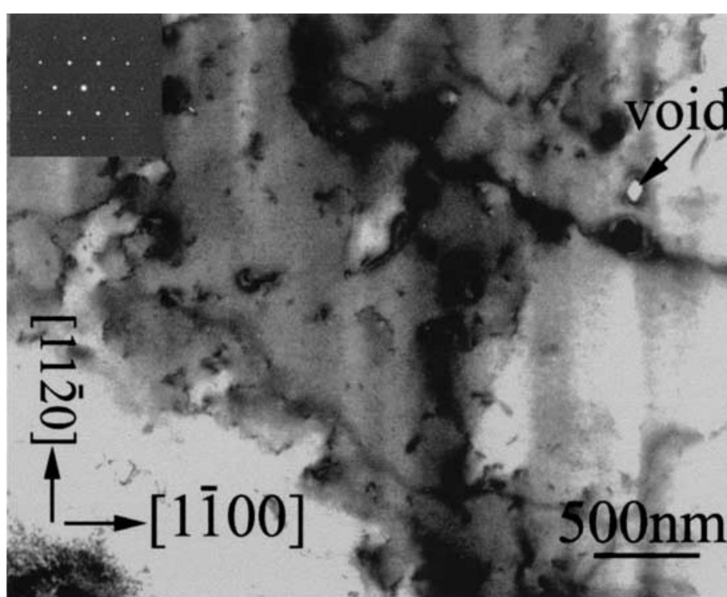

(a)

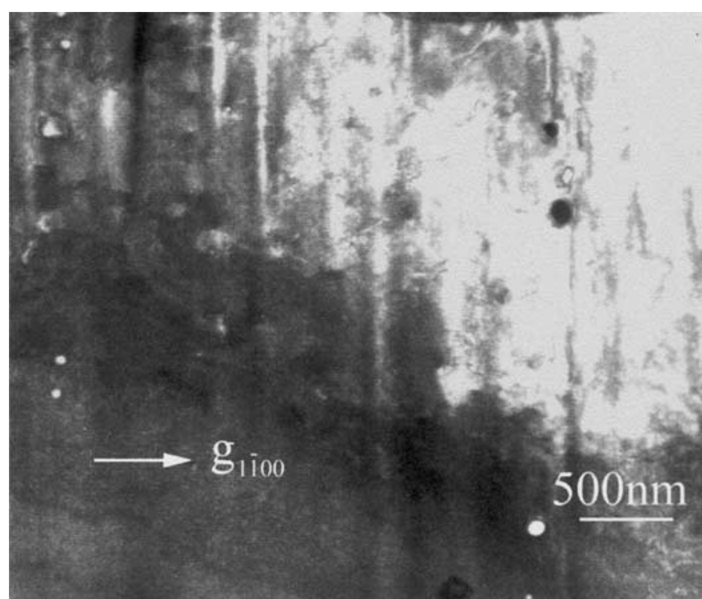

(b)

Figure 3 (a) Bright field plan view TEM image taken at the I site in Fig. 2(b) depicting the threading dislocation within (0001) plane, dark dots and segments correspond to end-on view of threading screw and complex dislocations respectively. The inserted is an selected area electron diffraction pattern. (b) Dark field image obtained using the ⟨1$\bar{1}$00⟩ reflections confirms the defects highly dominated by the screw dislocations.

TABLE I Morphological characterization of the epitaxial GaN

Width of strip (micron)	Coalescence of GaN		Orientation of the sidewalls	
	$[1\bar{1}00]$ strips	$[11\bar{2}0]$ strips	$[1\bar{1}00]$ strips	$[11\bar{2}0]$ strips
2	Yes	Yes	–	–
4	Yes	Yes	$\langle 11\bar{2}1 \rangle$	$\langle 1\bar{1}00 \rangle$
8	No	No	$\langle 11\bar{2}1 \rangle$	$\langle 1\bar{1}00 \rangle$
16	No	No	$\langle 11\bar{2}1 \rangle$	$\langle 1\bar{1}00 \rangle$

located at the window area of SiO_2 pattern are imaged. Dark field technique was adopted for determination of the dislocation type. Images were taken using different reflections. Most of these threading dislocations are out of contrast in dark field images obtained using $1\bar{1}00$ and $11\bar{2}0$ reflections. Threading dislocations in this region are mainly screw dislocations with Burgers' vector of 1/6[0001] type and dislocation lines extend along the [0001] direction [12–13]. These end-on threading dislocations are imaged as dark dots or segments in the plan view TEM image and often accompanied by bend contours. Threading dislocations initialize from the interface of GaN and alumina substrate and propagate through the windows of overgrown region. The arrangement of threading dislocation in the window area is uniform. These threading dislocations with a screw feature act as steps source along the normal to the (0001) growth plane [13].

Plan view image (Fig. 4) taken at the II position in Fig. 2b shows a typical dislocation arrangement. The

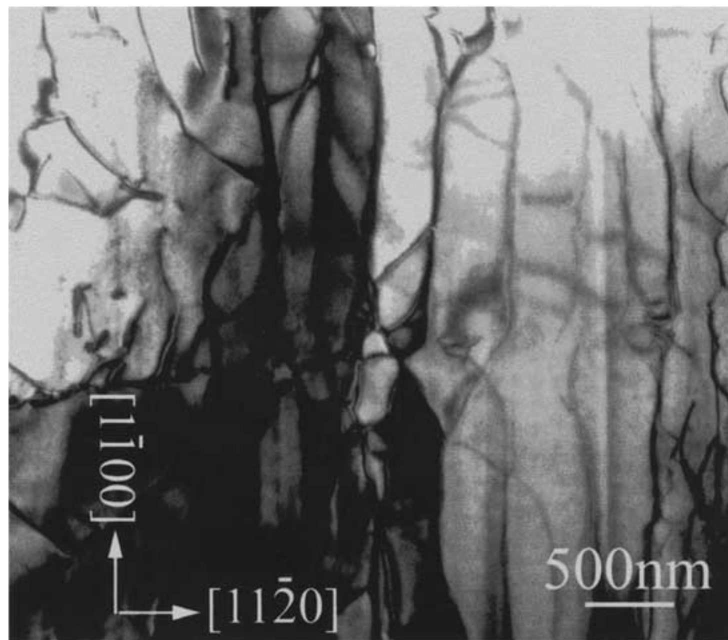

(a)

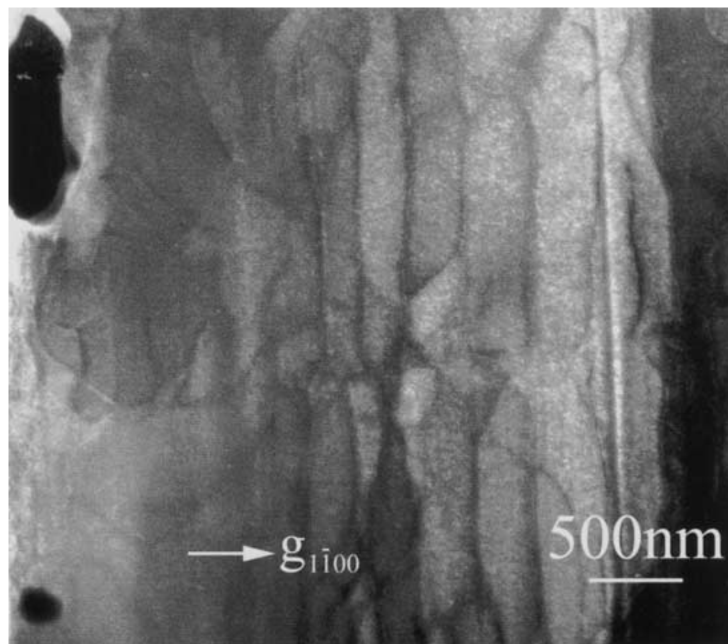

(b)

Figure 4 (a) Plan view image obtained at the II position in Fig. 2(b) illustrating evolution of dislocation network within the overgrown region, The dislocations mainly extend along the $[1\bar{1}00]$ direction. (b) Dark field image obtained using the $\langle 1\bar{1}00 \rangle$ reflection shows the dislocations coincident with edge dislocation.

dislocation configurations are very different from those in Fig. 3a. The characteristic feature of the dislocations in Fig. 4a consists of long straight segment, large loops and half loops. Because the strain fields are different for different kinds of dislocations, the types of these dislocations in Fig. 4a are determined by dark field technique. The long dislocation segments elongated in the $[1\bar{1}00]$ direction have a Burgers' vector of $1/3[11\bar{2}0]$ and coincide with edge type. Those dislocations extending along the other directions have a Burgers' vector of $1/3\langle 11\bar{2}3\rangle$ and contain a screw component. They are coincident with the reported results [9–11]. The dislocations in the overgrown area are initialized from change of the threading dislocation lines in window areas of the pattern. Due to SiO_2 mask aligned along the $[11\bar{2}0]$ direction, the lateral overgrowing fronts developed along the $[1\bar{1}00]$ direction and the threading dislocations also followed the overgrowing fronts and bent from the [0001] to $[1\bar{1}00]$ and other directions respectively, but majority to the $[1\bar{1}00]$ direction. Such a variation in dislocation lines also changed Burgers' vector from 1/6[0001] to $1/3[11\bar{2}0]$ and $1/3[11\bar{2}3]$, which resulted in the edge and mixed dislocations respectively.

In the overgrown region the dislocations mainly developed along the $[1\bar{1}00]$ direction for the mask strips aligning in the $[11\bar{2}0]$ direction. The dislocations supply the favorable locations for segregation of excess point defects and impurities present in this material. The dislocations charged by aggregation of point defects and electrical impurities along the extending lines can act as coulomb scattering centers, which scatter the carriers. The voids and nano-pipes could also act as the scattering centers of the carriers due to the presence of dangling bonds on their surfaces. The observed dislocations in LEO GaN would results in directional scattering of carriers. Scattering section in this case is a function of orientation angle. The maximum and minimum scattering sections are along the $[11\bar{2}0]$ and $[1\bar{1}00]$ directions respectively. Carriers would be scattered most strongly when moving along the $[11\bar{2}0]$ direction and less affected along the $[1\bar{1}00]$ direction. Directional scattering of the carriers and electrons by the locally charged dislocation network in GaN leads to anisotropy in carriers and electron mobility [4, 5]. Consequently, high concentration of dislocations could severely degrade the electric and optical qualities of the GaN film.

4. Concluding remark

The experimental evidence implies that a direct dependence of the sidewalls on the orientations of mask strips. The $\langle 1\bar{1}01\rangle$ and $\langle 11\bar{2}0\rangle$ aligned strips could alternatively result in the sidewalls coincident with the $\{11\bar{2}1\}$ planes that would introduce the surface with V-type voids and the $\{1\bar{1}00\}$ planes that would lead to the surface with rectangular voids. In the masked region the dislocations mainly extending along the $\langle 1\bar{1}00\rangle$ direction could result in an anisotropy in transverse mobility due to the directional scattering of the carriers by the charged dislocation lines. The voids and nano-pipes at the positions where the LEO GaN coalesced are also the favorable positions for formation of the scattering centers of the carriers due to the dangling bonds present at their surfaces.

The information from the SEM observations contributes to an increased understanding of the role of the lateral growth conditions on the morphological response. Combination of the mask strip's widths and directions together with the growth conditions makes it possible to improve the GaN quality and optimize the surface morphology and, thus, permit a basis for the design of the surface pattern. As a result it may be considerably beneficial for the optoelectronic devices manufacture process.

References

1. S. NAKAMURA, M. SENOH, S. NAGAHAMA, N. IWASA, T. YAMADA, T. MATSUSHITA, Y. SUGIMOTO and H. KIKOYU, *Jpn. J. Appl. Phys.* Part 2, **36** (1997) L1059.
2. S. J. PEARTON, J. C. ZOLPER, R. J. SHUI and F. REN, *J. Appl. Phys.* **86** (1999) 1.
3. D. P. FENG, Y. ZHAO and G. Y. ZHANG, *Phys. Status Solidi A: Appl. Res.* **176** (1999) 1003.
4. N. G. WEIMANN, L. F. EASTMAN, D. DOPPALAPUDI, H. M. NG and T. D. MOUSTAAKAS, *J. Appl. Phys.* **83** (1998) 3656.
5. Y. F. WU, B. P. KELLER, P. FINI, S. KELLER *et al.*, *IEEE Electron Device Letter* **19** (1998) 50.
6. J. A. JR. FREITAS, O. H. NAM, T. S. ZHELEVA and R. F. DAVIS, *J. Cryst. Growth* **189** (1997) 92.
7. J. S. SPECK and S. J. ROSNER, *Phys. B: Cond. Matter.* **273** (1999) 24.
8. R. JONES, J. ELSNER, M. HAUGK *et al.*, *Physica Status Solidi A: Applied Research* **171** (1997) 167.
9. R. JONES, *Materials Sci. Eng.* **B71** (2000) 24.
10. F. BERTRAM, J. CHRISTEN, M. SCHMIDT, M. TOPF *et al., Mater. Sci. & Eng. B: Solid-State Mater.* **50** (1997) 165.
11. S. C. JAIN, K. PINARDI, H. E. MAES, R. VAN OVERSTRAETEN, M. WILLANDER and A. ATKINSON, *Mater. Res. Soc. Sym. Pro.* **482** (1997) 875.
12. X. J. NING, F. R. CHIEN, P. PIROUZ, J. W. YANG and M. ASIF KHAN, *J. Mater. Res.* **11** (1996) 580.
13. W. QIAN, M. SKOWRONSKI, M. DE GRAEF, K. DOVERSPIKE, L. B. ROWLAND and D. K. GASKILL, *Appl. Phys. Lett.* **66** (1995) 1252.
14. R. HULL, J. C. BEAN, R. E. LEIBENGUTH and D. J. WERDER, *J. Appl. Phys.* **65** (1989) 4723.
15. R. ANDERSON, *Microsc. Microanal.* **4** (1999) 467.

Received 5 October 2001
and accepted 30 January 2002